



Canadian Geotechnical Journal
Revue canadienne de géotechnique

Field Performance of In-service Cast Iron Water Reticulation Pipe Buried in Reactive Clay

Journal:	<i>Canadian Geotechnical Journal</i>
Manuscript ID:	cgj-2014-0531.R2
Manuscript Type:	Article
Date Submitted by the Author:	29-Apr-2015
Complete List of Authors:	Chan, Derek; Monash University, Dept of Civil Engineering Gallage, Chaminda; Queensland University of Technology, Rajeev, Pathmanathan; Swinburne University of Technology, Civil and Construction Engineering Kodikara, Jayantha; Monash University,
Keyword:	Field instrumentation, cast-iron water main, soil movement, expansive soil, meteorological conditions

SCHOLARONE™
Manuscripts

Field Performance of In-service Cast Iron Water Reticulation Pipe Buried in Reactive Clay

Derek Chan, Ph.D.
Researcher, Department of Civil Engineering
Monash University, VIC 3800, Australia
E-mail: derek.chan@monash.edu

Chaminda Pathma Kumara Gallage, Ph.D.
Senior Lecturer, School of Urban Development
Queensland University of Technology, QLD 4001, Australia
chaminda.gallage@qut.edu.au

Pathmanathan Rajeev, Ph.D.
Senior Lecturer, Department of Civil Engineering and Construction Engineering
Swinburne University of Technology, VIC 3122, Australia*
E-mail: prajeev@swin.edu.au

Jayantha Kodikara, Ph.D.
Professor, Department of Civil Engineering
Monash University, VIC 3800, Australia
Phone: +61-3-9905 4963
Fax: +61-3-9905 4944
E-mail: jayantha.kodikara@monash.edu (corresponding author)

*Formerly a researcher in Department of Civil Engineering, Monash University, VIC 3800, Australia

Field Performance of In-service Cast Iron Water Reticulation Pipe Buried in Reactive Clay

D. Chan, C.P.K. Gallage, P. Rajeev and J. Kodikara

Abstract

Field monitoring is an important means for understanding soil behaviour and its interaction with buried structures such as pipeline. This paper details the successful instrumentation of a section of an in-service cast iron water main buried in an area of reactive clay where frequent water pipe breakage has been observed. The instrumentation included measurement of pipe strain; pipe water pressure and temperature; soil pressure, temperature, moisture content and matric suction, as well as the meteorological conditions on site. The data generally indicated that changes in soil temperature, suction and moisture content were directly related to the local climatic variations. The suction and moisture content data indicated that the soil profile at the site down to around 700 mm, and probably down to 1000 mm, is affected by changes in surface weather, while soil conditions below this depth appear to be more stable. Analysis of pipe strain indicated that the pipe behaves like a cantilever beam, with the top experiencing predominantly tensile strains during summer. Subsequently, these trends reduce to compressive strains as soil swelling occurs due to increase of moisture content with the onset of winter.

Key words: Field instrumentation, cast-iron water main, soil movement, expansive soil, moisture content, meteorological conditions

Introduction

Failure of buried water pipes due to ageing is one of the major problems that does not only result in wastage of precious water but also creates significant disruption to communities and economic losses in many global population centres, including Australian towns and cities. Therefore, it is important to improve our understanding of the factors and mechanisms of pipe failures and develop improved pipe asset management models that can predict water pipe failures in order to plan for the rehabilitation, replacement, and failure mitigation strategies of pipe assets.

Local and global evidence showed that buried pipe failure is affected by climatic, soil, and pipe variables. Baracos *et al.* (1955) analysed the pipe breakage data of cast iron (CI) and asbestos cement (AC) water mains in the city of Winnipeg (Manitoba, Canada) for the years 1948 to 1953 and found that the monthly number of circumferential failures had a close correlation with seasonal climate changes. Mordak and Wheeler (1988) analysed failure data from four water authorities with a large inventory of AC pipes in the U.K. for the period from 1952 to 1982. It was found that higher annual pipe failure rates were recorded in areas with clay soils and most of the failures occurred in the dry summer months. Further, high incidences of circumferential failures in smaller diameter pipes were observed. The association between plasticity index and water pipe breakage observed by Hudak *et al.* (1998) suggests that expansive clay may play an important role in breakage of water pipes. An analysis of AC water pipe failure data from Regina, Canada for the period from 1980 to 2004 by Hu and Hubble (2007) showed that the highest annual breakage rate corresponded to the year with the highest rainfall deficit. Other studies (Habibian 1994; Karaa and Marks 1990; Goulter and Kazemi 1988; Kettler and Goulter 1985; Bahmanyar and Edil 1983; O'Day 1982) have also determined the cause of failure by

identifying correlations between pipe breaks and influential factors, such as pipe age, pipe diameter, soil corrosivity, temperature, water pressure, and external loads, showing that the behaviour of buried pipes is closely related to the physical, environmental and operational conditions. On the basis of information gathered, it is generally evident that small diameter pipes or reticulation pipes (generally in the order of 100 or 150 mm in diameter) are more affected by the reactive soils and climate influence.

Previous studies in Victoria, Australia (Ibrahimi 2005; Chan *et al.* 2007; Gould and Kodikara 2008) have shown that failure rates of water pipes rise markedly during summer and to a somewhat lesser extent during winter. The analysis of pipe failure data indicates that these effects are much more pronounced after a prolonged dry period (e.g. summer 2001/2002), highlighting the susceptibility of the existing pipe network to local climatic changes. Gould *et al.* (2009) conducted an analysis of water pipe failure data obtained from two water authorities in Victoria, Australia for the period from 1996 to 2006. This study suggested that the pipe failure rate increases as net evaporation increases. Net evaporation is negatively related to soil moisture content, indicating that soil moisture content decreases as net evaporation and pipe failure rate increase. A higher failure rate was observed for cast iron pipes which are the oldest, with the greatest length of service, buried in expansive soils, and with diameters of 100 to 150 mm. Further, the study revealed that the rate of circumferential fractures increases with increase in net evaporation.

In spite of the effects of local climate, soil water content, temperature, pipe material, and pipe diameter on the performance of buried pipes, particularly in reactive soils, little work has so far been carried out to study the behaviour of buried pipes subjected to climate changes. Although some theoretical and numerical models were developed

to quantify the pipe-soil interaction effects (e.g., Rajani *et al.* 1995; Kuraoka *et al.* 1996; Rajeev and Kodikara 2011), the existing models consider only some of the physical variables, and the influence of soil and climate are not properly taken into account. Quantitative understanding of soil-pipe interaction would enable engineers to improve the design, construction, maintenance and management of buried pipes in reactive soils. Therefore, a field study was initiated involving the instrumentation of an in-service water main and surrounding soil in order to monitor the performance of pipe buried in reactive soil and subjected to seasonal climate variations. This is one of the rare instances where an in-service cast iron pipe buried in reactive has been monitored for over three years period. Since most world's urban centres including in Australia still has a more than 50% of water pipes as cast iron pipes, this study is significant to proactive management of the vital water and gas pipe network. This research provides on the basis of field measurement the likely mechanism that operates in the failure of these pipelines. This information should help devising rational methodologies to make failure forecasts and manage the pipe network.

This paper reports the details of the field instrumentation and the results of the pipe strain, soil water content, soil suction, and soil temperature measured over the monitoring period started from January 2008 and the pipe and soil response to weather change.

Field Instrumentation

Site selection criteria

A statistical analysis of water pipe failure data (Gould and Kodikara 2008) reported that 100 mm nominal diameter cast iron pipes are the most numerous assets in the water pipe network in north-western Melbourne, and these pipes experience failure

rates higher than those of other pipe materials and diameters. Of this pipe type, those located in reactive soils have the highest failure rate. Similar results were reported by Chan et al. (2007), who found that over 50% of pipe failures are in cast iron pipes and about 60% of the failed pipes were 100 mm diameter. For these reasons, it was decided to undertake the instrumentation on a 100 mm cast iron water pipe buried in reactive soil. The site was chosen following the criteria described below in order to be effective, safe, convenient, and least complicated for excavation, instrumentation and data-logging. The selection criteria for a suitable site were: an area with a history of high failure rates; a reactive soil region; contains a buried cast iron water pipe with nominal diameter between 100 to 150 mm; no previous failures have occurred within the instrumentation pipe length; pipe laid across nature strip and driveway to study the effects of pervious and impervious surfaces on buried pipe behaviour; wide nature strip to allow for instrumentation; clear of other utilities such as gas, power, telecommunications, storm water and sewer; relatively flat ground surface to avoid the effects of sloping ground and risk of potential flooding; no trees on the nature strip within and close to the instrumentation locations; and a quiet area with relatively low traffic flow.

A large number of sites were screened with the above criteria and two most suitable sites were chosen for additional investigation to determine soil depth and site-specific properties. According to the AS 2870 for residential slab and footing design (Standards Australia 2011), the change of suction depth in the Melbourne area is from ground surface to the depth of 1.8 m to 2.3 m. The possible ground movement due to climate may expect to occur within this depth. The field scale moisture measurement at 23 sites in Melbourne reported in Kodikara et al. (2014) reported that observed moisture changes are within 1.0 to 1.3 m. Soil investigations were done by hand

auguring and undisturbed push-tube sampling with a drill rig in order to determine the depth of soil at these two sites. The site chosen for instrumentation is located in Altona North, Victoria, Australia. This site has a clay layer of over 1.5 m depth below the ground surface.

Soil profile

Undisturbed soil samples were collected from the site by pushing 100 mm diameter pipes down to 2.1 m below the ground surface where the basaltic rock layer was found. The soil samples were then sealed on site to prevent moisture evaporation and brought to the laboratory for classification tests. In the laboratory, soil cores were extracted from the plastic tubes and soil samples were taken at different depths for measurement of moisture content, dry density, Atterberg limits, linear shrinkage, swelling pressure, saturated hydraulic conductivity, and soil-water characteristic curves (SWCCs). Table 1 summarises the physical properties of the soil with depth. The Atterberg limits test results on the plasticity chart are shown in Figure 1. The consistent clay soil found below the depth of 250 mm is classified as inorganic clays of high plasticity. The specific gravity of the soil collected at pipe depth (850 mm) was measured as 2.66. The particle size distribution test plotted in Figure 2 shows a high content (60%) of clay in the soil. The mineral composition of the soil collected at pipe depth was determined using the commercial package SIROQUANT for X-ray diffraction (XRD) (Srodon et al. 2001), and the results are shown in Table 2. A significant presence of clay minerals, including smectite, imparts high reactivity to the soil.

Soil samples taken at different depths were tested in an oedometer to determine the swelling pressures which varies from 110 to 600 kPa. This variation may be affected predominantly by the initial water content and initial dry density of the sample.

The saturated hydraulic conductivity of the topsoil was measured in the field using an air entry permeameter. Undisturbed soil samples collected at depths of 450 mm and 800 mm were used in the laboratory testing using the constant head method with flow pumps.

The relationship of volumetric moisture content and matric suction (SWCC) of the soil at various depths was measured by the filter paper method and the results are shown in Figure 3. The experimental data were fitted using the equation proposed by Fredlund and Xing (1994). The soil profile of the site is shown in Figure 4.

Pipe conditions

According to the records of the water authority, the 100 mm diameter cast iron pipe to be instrumented was installed in 1961. Given the installation date, it is likely that the pipe has an internal cement lining applied in the factory at the time of manufacture. During the field instrumentation, a non-destructive test was performed using an ultrasonic gauge to measure the pipe wall thickness. Twelve measurements taken at the pipe top, bottom and spring line on opposite sides in each of the three pits revealed that the average wall thickness of the pipe was 8.5 mm. The pipe crest is located at a depth of 850 mm below the ground surface.

Site plan

The plan view of the instrumentation site with locations of the access pits is shown in Figure 5. The total length of the nature strip between two driveways is 23.8 m and the

width between road and footpath is 4.8 m, which provided sufficient working area for instrumentation on the soil and pipe. In addition to the water pipe to be instrumented, which is located 3.16 m from the property boundary, a 100 mm diameter gas pipe is located 2.4 m from the property boundary and a storm water pipe is located 0.6 m from the kerb. Power and telecommunications lines are located 6 m overhead.

Field monitoring system installation

Pipe and soil instrumentation was undertaken in three primary locations, designated as Pit 1, Pit 2 and Pit 3 (Figure 5). Each pit contained two sections; a smaller section for instrumentation of the pipe, which was excavated to 1.3 m below the ground surface; and a larger section for instrumentation of the surrounding soil, which was excavated to 2.5 m below the ground surface. As shown in Figure 5, Pit 1 is located beneath the driveway, Pit 2 is 3.65 m to the right of the driveway (5 m to the right of the centre of Pit 1) and Pit 3 is 14.25 m to the right of the driveway (15.6 m to the right of the centre of Pit 1). An additional pit was located 3.4 m from the centre of Pit 3 for the installation of pipe water pressure and temperature gauges. These locations were selected to monitor the strain of the pipe, assuming that it behaved like a restrained end beam between the two driveways. In this case, Pit 1 was considered as the end of the “beam”, Pit 3 was considered near the mid-span of the “beam” (the location was shifted marginally due to the service pipe connection, as shown in Figure 5) and Pit 2 was at approximately one third of the distance between Pit 1 and Pit 3.

Numerous sensors and systems were installed on site to monitor the behaviour of pipe, the surrounding soil, and the weather conditions. The sensors included 12 biaxial strain gauges on the pipe surface for measurement of pipe deformation; 15 thermocouples for measurement of soil temperature; 15 thermal conductivity sensors

for measurement of soil suction; 15 soil moisture sensors (similar to time-dependent reflectometry (TDR) probes) for measurement of volumetric soil moisture content; two earth pressure cells to measure the soil pressure at the pipe-soil interface; a water pressure and temperature gauges on the pipe; weather station for measurement of the temperature, rainfall, humidity, wind speed and solar radiation on site; and three sacrificial anodes connected to the instrumented pipe sections to reduce pipe corrosion in order to protect the strain gauges. Figure 6 shows the vertical section layout of the sensors that were installed in this project. Note that the thermal conductivity sensors, soil moisture sensors and thermocouples were installed above and below the pipe by drilling horizontally through the soil from the larger section of each pit.

Majority of the fieldwork was undertaken between 7th and 14th January, 2008. The locations of each pit were marked and excavated. Shoring was then set up in the larger section of each pit to provide access and protect against collapse of the soil during sensor installation. During the excavation, spoil from each pit was marked as separate piles and returned to the same pit during backfill.

General-purpose 3-wire waterproof biaxial strain gauges (KFW-5-120-D16-11 from Kyowa, Japan) were installed to measure the deformation response of the pipe. These gauges are thermally-compensated with a thermal expansion coefficient of $11 \mu\epsilon/^{\circ}\text{C}$, which is similar to cast iron (Rajani *et al.* 1996; Sadiq *et al.* 2003). The smaller section of Pits 1, 2 and 3 exposed the water pipe for strain gauging and to allow installation of pressure cells underneath the pipe (Figure 7 and 8). In total, twelve strain gauges (three sets of four biaxial strain gauges) were installed. Each biaxial gauge consisted of two gauges: one gauge was oriented along the longitudinal axis of

the pipe to measure the longitudinal strain and the other gauge was oriented perpendicular to the first gauge to measure the circumferential strain. The strain gauges were attached to the pipe with special adhesive and proper waterproofing protection was applied. The strain gauge readings recorded after completion of backfill (at 12.30pm on the 12th January, 2008) were taken as the base values to initialise the rest of the results.

The pressure applied to the pipe by soil swelling and shrinkage was measured using the Geokon model 4800 vibrating wire earth pressure cells with 1 MPa capacity. The earth pressure cells were installed at locations directly beneath the pipe by digging a small hole in the wall of the pit beneath the pipe. A 15 mm thick, 200 mm diameter steel plate was then placed on the top of each pressure cell to ensure that the soil pressure was uniformly distributed on the pressure cell (Figure 8). The pressure cells were only installed in Pits 2 and 3 (Figures 5 and 6) as the change of soil pressure in Pit 1 (under the driveway) was expected to be minimal due to the low exposure to the prevailing weather conditions.

The pipe water pressure and temperature were monitored using SITRANS pressure and temperature gauges manufactured by Seimens with the ranges of pressure and temperature gauges of 0 to 10 bar and -50 to + 200 °C, respectively. These gauges were installed using custom-built T-pieces and tapped to the water pipe. The gauges were then enclosed in a plastic box with a removable top plate which was level with the ground surface and used to provide constant access to the gauges if required. Figure 9 shows the water pressure and temperature gauges installed on site.

Fifteen Type T thermocouple burial sensors (105T-L) were installed in the ground to monitor the soil temperature at various depths. All the thermocouples were tested in

the laboratory by being immersed in water of known temperature prior to installation in the field.

Fifteen Campbell Scientific 229 thermal conductivity sensors were installed on site to measure the matric suction profiles of the soil. The sensor is designed in such a way that it is in equilibrium with the surrounding soil suction, and therefore after calibration it can measure the suction prevailing in the surrounding soil.

Fifteen ML2x soil moisture content sensors manufactured by Delta-T Devices were installed on site. These sensors were calibrated using soil samples collected from the instrumentation site.

The thermocouples, suction sensors and moisture content sensors were installed at four different levels in smaller sections of Pit 1, 2 and 3 as shown in Figure 6. In Pit 3, a fourth set of sensors was installed at three levels in the pit away from the pipe, towards the road. These sensors were installed to monitor the soil at the road-side for comparison with the measurements made at the pipe profile.

After the instrumentation, all pits were backfilled using the original material and compacted to a density close to the initial density (i.e. the same amount of soil excavated from each pit was used to backfill). However, no in-situ density measurements were conducted. The soil was compacted in four to five layers up to the ground level, and each layer of loose soil was sprayed with water before compacting with a vibrating plate compactor. In error, a large amount of water (more than necessary for compaction) was poured into Pit 3 to wet the bottom soil layers prior to compaction of the layer above them. This should be noted when viewing the analysis of sensor information.

The top 300 mm of Pit 1 (under the driveway) was backfilled with crushed rock and a temporarily driveway was created using bitumen. A new driveway was installed

several weeks after the fieldwork was completed. The nature strip was reinstated after the instrumentation. The amount of water used to support grass growth is not known. Supplementary fieldwork was undertaken on 19th February for the installation of the Campbell Scientific weather station. It consisted of a tipping bucket rain gauge (CSI Model CS700) with a measuring range of 0 to 500 mm/hr and resolution of 0.254 mm, an anemometer for wind speed measurement with a range of 0 to 50 m/s and resolution of 0.5 m/s, a pyranometer (LI200X) to measure solar radiation, and a HMP50 temperature and relative humidity sensor. The weather station was attached to a galvanized steel pipe connected to the instrumentation cabinet such that the weather station was located 4.5 m above the ground surface. Figure 10 shows the weather station after installation and its components.

All sensors, with the exception of the weather station, were connected to the Campbell Scientific CR 1000 datalogger and its peripherals. The CR 1000 datalogger was programmed using a customized logging program (written in CRBasic) provided by Campbell Scientific. The weather station sensors were connected to a CR 800 data-logger, which has a similar program to the CR 1000. The data were acquired at intervals of 10 minutes.

Results and discussion

The analysis and discussion of the data collected from the field instrumentation are presented in this section. The data presented in this paper were collected over three years between 12th January, 2008 and 13th February, 2011.

Pipe water pressure

Figure 11 shows the fluctuation of pipe water pressure for the three weeks from 7th to 27th April, 2008. A cyclical pattern of water pressure fluctuation is observed, where the maximum pressure of 754 kPa and the minimum pressure of 650 kPa are indicative. A plot of the average water pressure on weekdays and weekends during this period is shown in Figure 12. The maximum daily pressure was seen at approximately 5:00am. A significant pressure drop can be observed from 6:00am to 9:00am on weekdays, likely due to the morning activities of the residents. A similar but slightly smaller pressure drop is also seen on weekends 1.5 hours later than on weekdays. The water pressure then increases until 6:00pm, before a second decrease, although to a significantly lesser extent than that seen in the morning, from 6:00pm to 8:00pm, likely coinciding with the evening activities of the residents.

Soil pressure

The two earth pressure cells installed at Pits 2 and 3 showed different responses, as shown in Figure 13. The average moisture content measured at 700 and 1000 mm beneath the nature strip, and the calculated overburden pressure at the depth of the pressure cells (at 0.85 m based on soil density and depth) are also shown. The earth pressures recorded in both pits showed similar trends but with different magnitudes of change. The earth pressure in Pit 2 appeared to have a more realistic response, and the lower magnitudes of change at Pit 3 may be due to poor soil compaction around the pressure cell. Nevertheless, both pressure cells responded to the change of soil moisture content. More detailed analysis of the responses from the earth pressure cells focuses on the results from Pit 2.

The pressure recorded in Pit 2 was seen to increase between January and March 2008, where decrease in soil moisture content is recorded. At the end of April 2008, soil moisture started to increase until September 2008, when a decrease in soil pressure was recorded. These results are somewhat intriguing, as it was expected that soil pressure would increase with soil moisture content when swelling of soil occurred. However, following the soil pressure recorded in the monitoring period, soil pressure peaked in March 2008, 2009 and 2010 when soil moisture was at minimum. In contrast, decrease in soil pressure was recorded in September 2008 and 2009 when soil moisture was maximised. Following this behaviour, it can be identified that increase of soil moisture content which can lead to swelling of soil is measured as a decrease in soil pressure, and shrinkage of soil due to a reduction in moisture content is recorded as an increase in soil pressure.

A possible explanation to this behaviour is that the pressure cells installed on site did not measure the pressure of the soil immediately beneath the pipe, but the pressure exerted by soil close to the pipe. When moisture content decreases, shrinkage of soil caused an increase in soil density and hardening, giving rise to higher effective stress due to capillary forces. Therefore, it was possible for the pressure exerted on the cell to increase. The pressure drop seen in September due to the increase of soil moisture content can also be explained by this mechanism, as the pressure due to shrinkage would be released when soil swelling and softening occurs.

The recorded soil pressure fluctuations suggest that soil swelling and shrinking occurred over the period with respect to the seasonal climate change. When soil pressure increased during drying and subsequently decreased during wetting, additional stresses were imposed on the pipe due to soil movement around the pipe.

Variation of soil pressure is a cyclic behaviour related to climate change in soil moisture content.

Moisture content and suction

The matric suction and moisture content of the soil were measured at four different depths by the sensors installed at each pit. As the measurement in the nature strip at Pit 2 and 3 was similar, only the data in Pit 1 under the driveway and Pit 2 are reported in this paper.

Figures 14 (a) and (b) show the matric suction and moisture content with time for Pit 1 (under the driveway) and Pit 2 (in the nature strip), respectively. Whilst data were logged at ten-minute intervals, the results in these figures show daily average values. The daily rainfall is also plotted in each figure to provide comparisons with the rainfall. The responses of soil moisture sensors (SMSs) appeared to be more consistent with the recorded rainfall data than the thermal conductivity sensors (TCSs). This is not surprising, as the TCS sensors are less robust than the SMSs in operation.

Figure 14 (a) shows the response of the sensors at Pit 1 (1 to 4), under the impermeable driveway. The response of sensors to rainfall is not immediate as the soil is not directly exposed to the atmosphere, and the delay of the response may be around one to two months, depending on the depth and conductivity of the soil. The TCS1 at 300 mm depth showed an increase in suction after instrumentation until the rainfall in February 2008, after which a sharp decrease in suction can be observed. Consistent with this, the SMS1 installed at the same depth also showed an increase in moisture content. Subsequently, TCS1 seems to have responded to main rainfall events during the data collection period, while increasing in suction during other

times. Similar response can be observed in SMS1 with moisture change following the rainfall events. The TCS2 at 550 mm depth shows a more subtle response to individual rainfall events, but with seasonal cyclic suction peaks throughout the years. This seems to be in agreement with the response of SMS2 installed at the same depth, which also showed seasonal peaks in moisture content. SMS 3, TCS3 and SMS4, TCS4 installed at 1000 mm and 1750 mm depths respectively, showed clearer seasonal cyclic behaviour than the sensors at 550 mm with soil moisture at a minimum in September and maximum in March, except at the end of 2010, when the soil moisture at these depths also increased over the extended rainfall period. The data suggest that soil at these depths that is under a relatively impervious surface, such as a driveway, is normally unaffected by surface weather conditions, specifically in reference to the moisture content and matric suction which influence soil movement. Figure 14 (b) shows the response of SMS and TCS at Pit 2 (5 to 8). The response to rainfall is more immediate at the natural strip, especially at 300 mm and 700 mm, as the TCSs respond to the rainfall events after instrumentation in March and May 2008 with the corresponding responses observed from the SMSs. The drop of suction at 300 mm depth (TCS5) corresponding to these rainfall events is not so significant. This may be due to surface cracks, which could have facilitated water flowing easily to deeper depths without much water retention at 300 mm depth. The suction at all depths showed a sharp reduction in late 2010, corresponding to the increase in moisture content, seemingly in response to the extended rainfall period. TCS 7 and 8 located at 1000 and 1750 mm depths respectively, showed similar responses to Pit 1, with suction peaking in September and minimised in February and March, corresponding to the minimum and maximum soil moisture contents measured at these depths.

In summary, the results from the SMSs and TCSs show change of soil suction and moisture content over the observation period in response to the weather recorded by the weather station. It is apparent that the soil profile down to 700 mm is closely affected by the surface conditions with respect to moisture change. Below this depth, soil conditions appear to change seasonally. Due to the low permeability of clay, the effect of surface wetting and at the depth below 700 mm is more subtle. It results in a seasonal cyclic variation of wetting and drying of soil, rather than a rapid response to climate events. According to the moisture content measurements, approximately 10% moisture content change can be expected at the pipe depth (850 mm). In general, higher water content and lower suction can be observed in soil under the driveway compared to the results in the nature strip. This could be caused by the different surface cover conditions of the driveway (concrete) and the nature strip (grass). Concrete cover will minimise soil moisture evaporation and rainwater infiltration below the cover and will maintain relatively high stable moisture content.

Anomalous behaviour of some sensors was noted, possibly due to the differences in initial moisture content at each pit or/and the malfunctioning of some sensors. It is observed that SMSs provide more robust measurement than TCSs, as the suction values will approach zero once moisture starts to increase. Another possibility is that the ground may have special structural features causing non-uniform water flow conditions. One such feature may be the presence of desiccation cracks.

The soil moisture content measured on site was used for numerical modelling and long term prediction of soil moisture and temperature was undertaken using the developed ground-atmosphere interaction model, details of this work is described in Rajeev et al. (2012).

Soil temperature

The temperature of the soil was measured at four different depths by the thermocouples installed at each pit. Similar to the moisture and suction measurement, only the data for Pit 1 and 2 are shown. Figures 15 (a) and (b) show the soil temperature for Pit 1 (under the driveway) and Pit 2 (in the nature strip), respectively, plotted with the variation of air temperature measured by the weather station and pipe water temperature by the temperature gauge connected to the pipe.

The data clearly show that when the soil is closer to the ground surface (i.e. 300 mm), it is more affected by the variation of air temperature, while the soil at greater depths (550 mm to 1750 mm) follows a more damped variation in temperature, but nonetheless is still influenced by the air temperature fluctuations. The effect of air temperature on soil temperature is most significant at Pit 1, as Figure 15 (a) shows that the soil temperature at 300 mm depth follows the daily fluctuation of air temperature more closely (varies from 9 °C to 31 °C) than the other locations. This may be due to TC 1 installed at Pit 1 being directly under the concrete driveway, which is more responsive to change of air temperature than the nature strip (as shown in Figure 15 (b), as the thermal conductivity of soil is less than that of concrete. TCs at greater depth had similar measurements, regardless of the pit location, and at 1000 mm the soil temperature is around 23 °C to 12 °C, while at 1750 mm the temperature varies from 22 °C to 14 °C.

The instrumented water pipe was located at 850 mm depth and TC6 and 7 at 700mm and 1000 mm respectively, can be used as an estimation of the possible temperature experienced by the water pipe. The soil temperature is affected by seasonal

atmospheric air temperature in such a way that in summer, the soil temperature decreases with the depth at an approximate rate of $2.5\text{ }^{\circ}\text{C/m}$ and in winter it increases with the depth at the same approximate rate. Further, the soil temperature at pipe depth could change by approximately $15\text{ }^{\circ}\text{C}$ from February to August, which could cause the development of significant thermal stress in the pipe. It is worth noting that the maximum soil temperature occurred during February and March, which is the same as the period when the maximum soil pressure was recorded, as shown in Figure 15. The influence of such temperature variation on the moisture change has been modelled in Rajeev *et al.* (2012).

Pipe strain measurement

Three sets of biaxial strain gauges were installed on the pipe; the detailed locations and labelling of the strain gauges are shown in Figure 16. Each of the pipe sections had four biaxial strain gauges, one on the top and the bottom and two at the spring line on opposite sides. Each of the biaxial gauges had one gauge oriented along the longitudinal axis of the pipe and the other gauge oriented perpendicular to the longitudinal gauge for measurement of hoop (or circumferential) strain. The location of the joints was based on the pipe joints being 6 m apart and the known location of a joint found under the driveway next to the first set of strain gauges during instrumentation.

Figure 17 shows the variation of the average longitudinal and hoop strains measured at each pit over time. The sign convention used is that tension is positive and compression is negative, following the traditions of structural engineering. The average strains were computed using the strain reading from all four strain gauges at each location. Therefore the strain due to bending of the pipeline is eliminated on the

basis of the assumption that the pipe bending follows the Euler–Bernoulli beam theory (i.e., strain due to bending varies linearly with equal and opposite sign at the top and bottom fibre of the section). As a result, the longitudinal strain shown in Figure 17 is the strain variation due to axial elongation/contraction of the pipeline. The soil temperature at the pipe depth is also shown in the figure, which in fact shows close correlation with the measured longitudinal strain variation. The soil temperature at the pipe depth was taken as the average of six thermocouples located above and below the pipe at three pits. In general, strain is maximum (tensile strain) in February to March and minimum (compressive strain) in August to September. This seasonal effect can be observed for over a year from the installation on January 2008 to March 2009. The strain gauges provided good measurements for approximately one year before some gauges started to give erratic data in April 2009. In general, the measured strains followed the trend of the soil temperature variation, but at later stage the tensile strain of all pits increased without any physical explanation. Some strain data had spikes that were not related to other strain measurements. It is believed that these gauges were malfunctioning and not giving reliable measurements, hence only the data from the period up to August 2009 were considered in the analysis.

Figure 18 illustrates a plot of differences in longitudinal strains measured at the top and the bottom of the pipe (i.e., longitudinal strain measured at pipe top subtract pipe bottom) at three pit locations with soil pressure and average soil moisture changes at 700mm and 1000 mm depths together with rainfall data. Using the strain measurements and the soil moisture variation as shown in Figure 18, the response of pipe buried in expansive soil subjected to climate can be explained with possible failure mechanisms.

As stated above, the joints are bolted joint and assumed to behave rigidly. Further, the soil moisture change within the driveway (i.e., close to pit 1) is not significant as in pits 2 and 3. Therefore, the soil movement under the driveway is very minimal and the joint close to pit 1 can be assumed as rigid support to rest of the pipe section. The pipe section in pit 2 and 3 behaves as a cantilever beam during soil swelling and shrinking with soil moisture changes. The flexural strain in Figure 18 was calculated by subtracting the longitudinal strain in the top and bottom of the pipe. The positive flexural strain in the figure suggested that the strain in the top is larger than the bottom, therefore pipe is bending downward according to cantilever action (i.e., pipe top is in tension). Conversely, the negative flexural strain suggested that the pipe is bending upward (i.e., pipe top is in compression). In order to understand the effect of climate in pipe behaviour, the seasons are signified in the figure with year.

At Pit 2 and 3 the strain values stabilised during the initial months after instrumentation, and then gradually decreased from autumn to winter 2008 (March to September/mid-November). It is clear that the soil moisture content increased during the same period of time, with the recorded decrease of soil pressure suggesting soil was swelling and the pipe bent upward. This was then followed by an increasing trend of strain which became positive, when the soil moisture content dropped over spring 2008 before a sudden rise in summer 2009. These trends can also be correlated to the increase in soil pressure during spring 2008, as the soil was shrinking. The influence of the dry summer in 2009 can be observed as the peaking of tensile strain on the pipe. There is a time lack of two to four weeks between the moisture change and corresponding soil response (i.e., soil pressure development).

A similar correlation can be also observed in Pits 1 such as, in autumn to winter 2008 and later part of Autumn to winter 2009, the decreasing trends of flexural strain was

observed with increasing soil moisture content and soil pressure. Decreases in strain (i.e., compression) and soil pressure and an increase in moisture content can be observed when approaching spring 2008 and winter 2009, showing swelling of soil in the wet season. Further, in summer to later autumn 2009, the flexural strain increased to maximum positive value while the average moisture was decreasing. This confirms that the pipe flexural strain is significantly high in either summer or autumn due to loss of soil support when soil shrinks.

According to the collected data during the monitoring period, it can be understood that soil shrinking occurred around summer due to the decrease of soil moisture content and increase in soil pressure. If the buried pipe is assumed to behave like a cantilever beam with partially fixed end support at the driveways (Chan 2008), the positive stress difference between the top and bottom of the pipe means the pipe top is in tension compared to the pipe bottom at the section under consideration. Hence, it is bending downward. When the stress difference between the top and bottom is negative, the pipe top is in compression compared to the pipe bottom, and therefore the pipe bends upward. Soil shrinkage in summer causes downward bending of the pipe in the nature strip with respect to that under the driveway, while the thermal effects in summer causes expansion of the pipe as shown in Figure 19. Due to possible rotation at joints, pipe segments bend downward and expanded, behaving like a beam subjected to uniformly distributed load and developing tensile strains on the top of pipe segments. In winter, wetting of soil pushes the pipe upward and this movement corrects the downward movement of the pipe that occurred previously, the pipe segments also contracted due to winter resulting in decreasing flexural strain (compression) at the top of the pipe.

It can be inferred from the strain analysis that in the monitoring period of two years, the pipe top experienced predominantly flexural tensile strain when the soil was shrinking during summer, and the strain was reduced eventually leading to compressive strain as the soil was becoming wetter, due to the increase of moisture content during winter. These field results are consistent with the findings of other studies (Ibrahimi 2005; Chan 2008; Gould & Kodikara 2008), where hot and dry summers were suspected of causing higher failure rates. It can also be inferred that shrinking and swelling of soil occurs due to the change of soil moisture content as a result of climate events (i.e. rainfall and evapo-transpiration). Bending of pipes is caused by climate events and upward and downward bending occurs with respect to the change in soil moisture content.

Conclusions

The following conclusions can be drawn from the analyses of field data described in this paper:

- The daily activities of residents caused approximately 80 kPa change in daily pipe water pressure. This change was consistent over the observation period.
- Change in soil pressure is subjected to moisture change, as soil pressure decreases with increase in soil moisture content, and vice versa. Maximum soil pressure at the pipe depth was recorded in March, while minimum soil pressure was recorded in September. The data are generally related to the corresponding swelling and shrinkage in soil wet and dry seasons.
- The change in soil moisture and suction are related to the prevail climate, including rainfall. The surface moisture change affects shallow depths (less than 1 m) in a relatively short time and deeper depths (greater than 1 m) with a

seasonal cyclic variation. Approximately 10% change in water content at the pipe depth can be observed.

- The soil temperature is closely related to the air temperature and the rates of temperature change with depth during summer and winter periods are about - 2.5 °C and + 2.5 °C per metre depth, respectively. The soil temperature decreases approximately in 15°C from summer to winter.
- The longitudinal and hoop strains of the pipe increase approximately 800 $\mu\epsilon$ (tensile) from winter to summer.
- The strain analyses show that tensile strain development at the top is correlated with decrease of soil moisture content and increase in soil pressure in summer. Compressive strain develops at the top when soil moisture content increases and soil pressure decreases when approaching winter.
- The analyses of strain suggest that during the monitoring period, the pipe moved downward in summer and upward in winter due to shrinking and swelling of soil respectively, as a result of the seasonal fluctuation of soil moisture content.
- Higher pipe failure rates recorded in Victoria during summer can be a result of downward bending of the pipe due to soil shrinkage.

Acknowledgements

This field instrumentation was conducted in co-operation with City West Water Limited (CWW), one of the major industrial partners of this ARC Linkage project. The authors would like to express their appreciation to CWW for their financial and in-kind support and assistance during this instrumentation. The authors would also like to thank the other partners: SP AusNet, Alinta Limited, Envestra Limited, South

East Water, Water Corporation, Ipswich Water, CSIRO and Queen's University (Canada) for their financial and in-kind support throughout this project. Finally, the authors would like to acknowledge the Australian Research Council (ARC) for being the main financial contributor to this project. The authors would also like to thank Scott Gould, Kok Yun Lee and Ben Shannon for their help during the field instrumentation.

References

- Bahmanyar, H.G., and Edil, T.B. 1983. Cold weather effects on underground pipeline failures. *In* Proceedings of ASCE Conference on Pipelines in Adverse Environments II, San Diego, California, 14-16 November 1983. American Society of Civil Engineers, New York, pp. 579-593.
- Baracos, A., Hurst, W.D. and Legget, R.F. 1955. Effects of physical environment on cast iron pipe. *Journal of American Water Works Association*, **42**(12): 1195-1206.
- Chan, D. 2008. Performance of water and gas pipes buried in reactive soil. M.EngSc. thesis, Department of Civil Engineering, The Monash University, Melbourne VIC.
- Chan, D., Kodikara, J. K., Gould, S., Ranjith, P. G., Choi, X. S. K., and Davis, P. 2007. Data analysis and laboratory investigation of the behaviour of pipes buried in reactive clay. *In* Proceedings of 10th Australia-New Zealand Conference on Geomechanics, Brisbane, Queensland, 21-24 October 2007. Australia New Zealand Conference on Geomechanics, Brisbane, pp. 206 – 211.

- Fredlund, D. G., and Xing, A. 1994. Equations for the soil-water characteristic curve. *Canadian Geotechnical Journal*, **31**(4): 521-532.
- Gould, S., and Kodikara, J.K. 2008. Exploratory Statistical Analysis of Water Reticulation Main Failures (Melbourne, Australia) Report RR11. Department of Civil Engineering, Monash University, Melbourne, VIC.
- Gould, S., Boulaire, F., Marlow, D., and Kodikara, J. 2009. Understanding how the Australian climate can affect pipe failure. *In Proceedings of the Australia's National Water Conference and Exhibition, OzWater 09 (CD-ROM)*, Melbourne, Victoria, 16-18 March 2009. Australian Water Association, NSW.
- Goulter, I.C., and A. Kazemi. 1988. Spatial and temporal groupings of water main pipe breakage in Winnipeg. *Canadian Journal of Civil Engineers*, **15**(1): 91–97.
- Habibian, A. 1994. Effects of temperature changes on water mains breaks. *Journal of Transport Engineering*, **120**(2): 312–321.
- Hu, Y., and Hubble, D. 2007. Factors contributing to the failure of asbestos cement water mains. *Canadian Journal of Civil Engineering*, **34**(5): 608-621.
- Hudak, P.F., Sadler, B., and Hunter, B.A. 1998. Analysing underground water-pipe breaks in residual soils. *Water Engineering and Management*, **145**: 15-20.
- Ibrahimi, F. 2005. Seasonal variations in water main breaks due to climate variability and ground movement. *In Proceedings of the Australia's National Water Conference and Exhibition, OzWater 05*, Brisbane, Queensland, 8-12 May 2005. Australian Water Association, NSW, pp. 28-35.
- Karaa, F.D., and Marks, D.H. 1990. Performance of water distribution networks: Integrated approach. *Journal of Performance of Constructed Facilities*, **4**(1): 51-67.

- Kettler, A.J., and Goulter, I.C. 1985. An analysis of pipe breakage in urban water distribution networks. *Canadian Journal of Civil Engineering*, **12**(2): 286-294.
- Kodikara, J. K., Rajeev, P., Chan, D. and Gallage, C. 2014. Soil moisture monitoring at the field scale using neutron probe. *Canadian Geotechnical Journal*, **51**(3): 332-345.
- Kuraoka, S., Rajani, B., and Zhan, C. 1996. Pipe soil interaction analysis of field tests of buried PVC pipe. *Journal of Infrastructure Systems*, **2**(4): 162-170.
- Mordak, J., and Wheeler, J. 1988. Deterioration of asbestos cement water mains. Final report to the Department of the Environment Report No. DWI0131, Water Research Centre, Swindon, Wiltshire.
- O'Day, K. D. 1982. Organizing and analysing leak and break data for making main replacement decisions. *Journal of American Water Work Association*, **74**(11): 589-594.
- Rajani, B., Zhan, C., and Kuraoka, S. 1996. Pipe-soil interaction analysis of jointed water mains. *Canadian Geotechnical Journal*, **33**(3): 393-404.
- Rajeev, P., and Kodikara, J. 2011. Numerical Analysis of an Experimental Pipe Buried in Swelling Soil. *Journal of Computers and Geotechnics*, **38**(7): 897-904.
- Rajeev, P., Chan, D., and Kodikara, J. K. 2012. Ground-atmosphere interaction modelling for long-term prediction of soil moisture and temperature. *Canadian Geotechnical Journal*, **49**(9): 1059-1073.
- Sadiq, R., Rajani, B. and Kleiner, Y. (2003). "Probabilistic risk analysis of corrosion associated failures in cast iron water mains." *Reliability Engineering and System Safety*, **86**(1): 1-10.

- Srodon, J., Drits, V.A., McCarty, D.K., Hsieh, J.C.C., and Eberl, D.D. 2001. Quantitative X-ray diffraction analysis of clay-bearing rocks from random preparation. *Clays and Clay Minerals*, **49**(6): 514-528.
- Standards Australia Limited. 2011. Residential slabs and footings AS2870. Standards Australia, Sydney, NSW.

Draft

Figure Captions

Fig. 1. Plasticity chart classifying the site soil

Fig. 2. Particle size distribution of the site soil

Fig. 3. Soil water characteristic curve for the site

Fig. 4. Soil profile of the site

Fig. 5. An instrumentation plan of the site

Fig. 6. Vertical section of instrumentation site

Fig. 7. Location of biaxial strain gauges around the pipe in a set

Fig. 8. Installation of an earth pressure cell

Fig. 9. Pipe water pressure and temperature gauges

Fig. 10. Weather station and its components

Fig. 11. Variation of pipe water pressure (collected in 10 min intervals)

Fig. 12. Average daily fluctuation of pipe water pressure

Fig. 13. Variation of soil pressure at Pit 2 and 3

Fig. 14. (a) The variation soil suction and moisture content in response to rainfall at Pit 1; (b) The variation soil suction and moisture content in response to rainfall at Pit 2

Fig. 15(a). Seasonal variation of soil temperature at Pit 1; (b) Seasonal variation of soil temperature at Pit 2

Fig. 16. Location and labelling of strain gauges on the pipe

Fig. 17. Development of longitudinal and hoop strain in response to pipe temperature

Fig. 18. Comparison of the difference between the top and bottom longitudinal strain gauges with soil pressure, displacement, moisture content and rainfall

Fig. 19. Vertical pipe movement due to seasonal climate change of soil moisture content

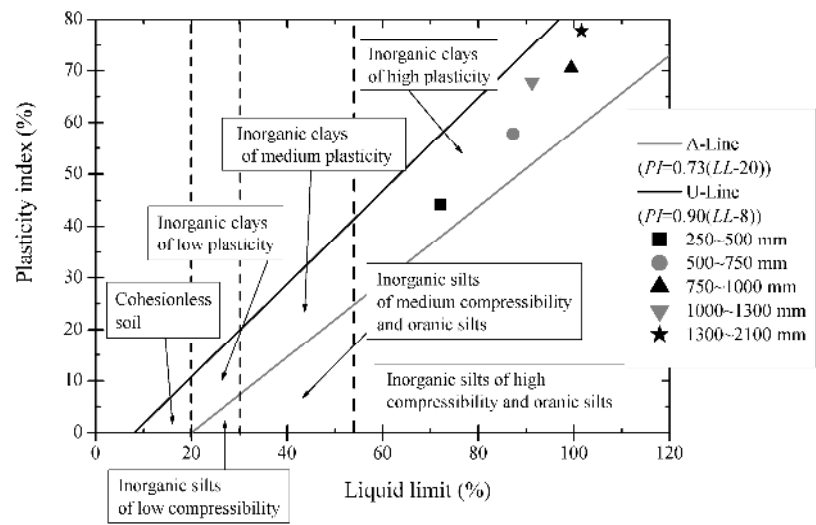


Fig. 1. Plasticity chart classifying the site soil
1236x874mm (72 x 72 DPI)

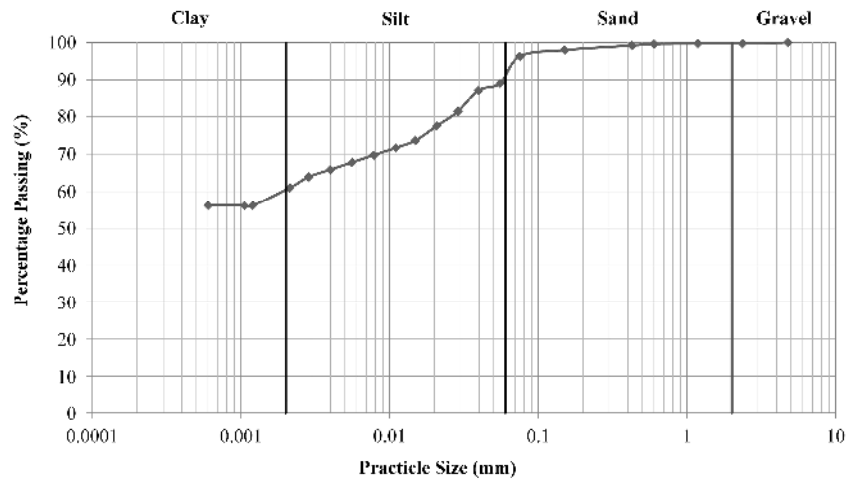


Fig. 2. Particle size distribution of the site soil
2473x1749mm (72 x 72 DPI)

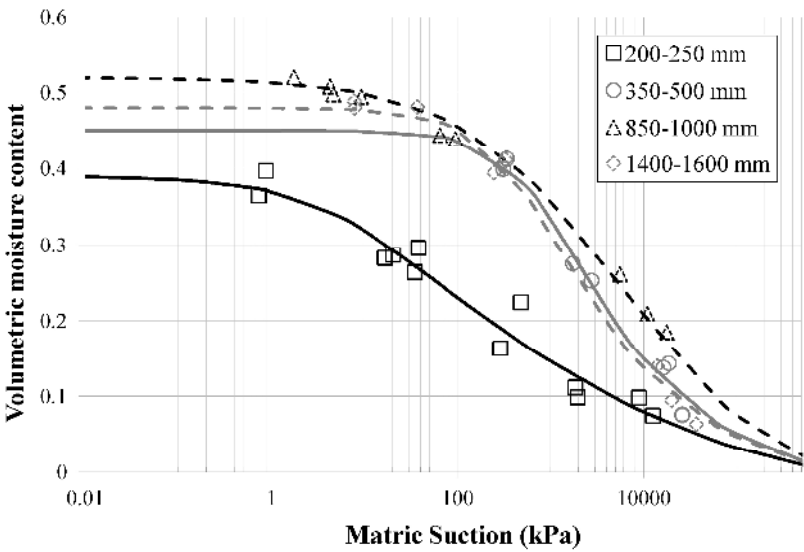


Fig. 3. Soil water characteristic curve for the site
1236x874mm (72 x 72 DPI)



Altona North			
Boring Method	Inferred Stratigraphy	Graphic Log	Depth (m)
			0.0
Push tube	Top soil: MH silty clay, dark grey with root fibers, dry to moist		0.4
	CH inorganic clay of high plasticity, dark to light grey, moist, stiff to very stiff		2.0
Rock core	Basalt rock		

Fig. 4. Soil profile of the site
146x219mm (300 x 300 DPI)

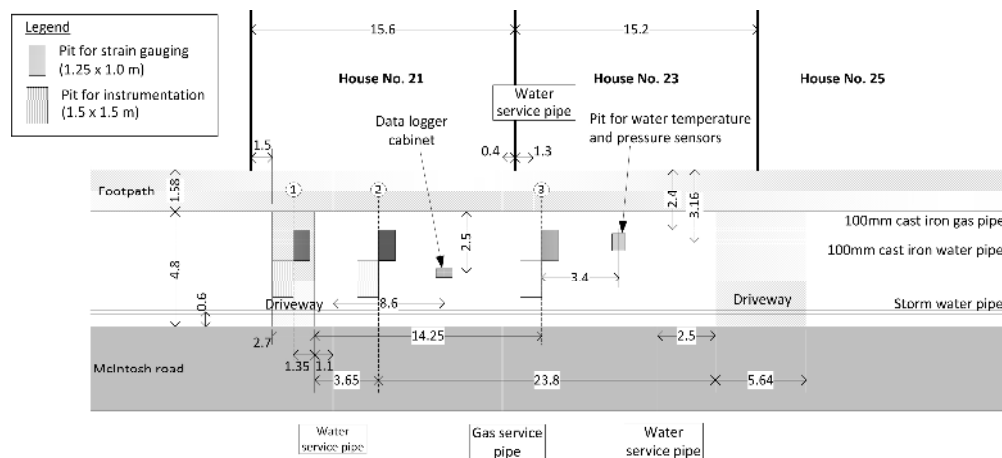


Fig. 5. An instrumentation plan of the site
825x372mm (96 x 96 DPI)

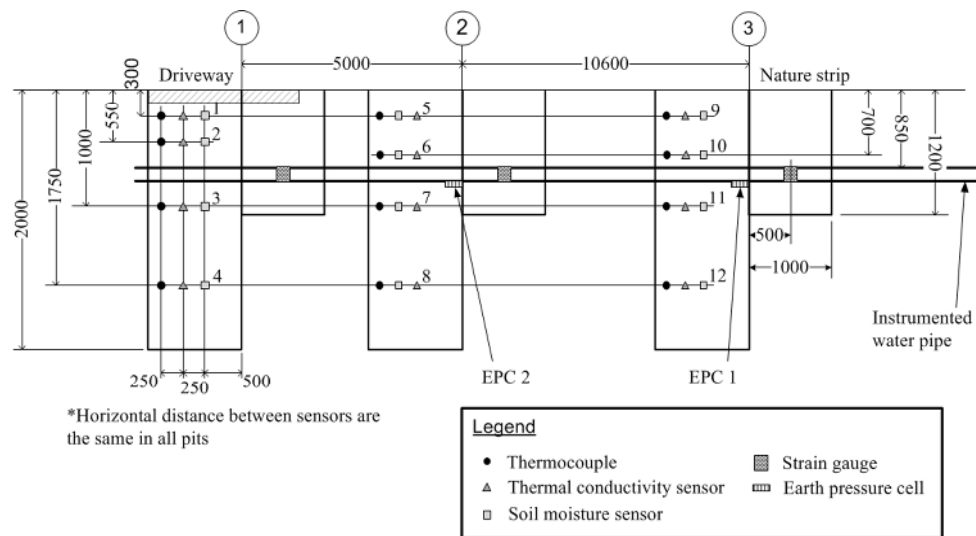


Fig. 6. Vertical section of instrumentation site
298x167mm (96 x 96 DPI)

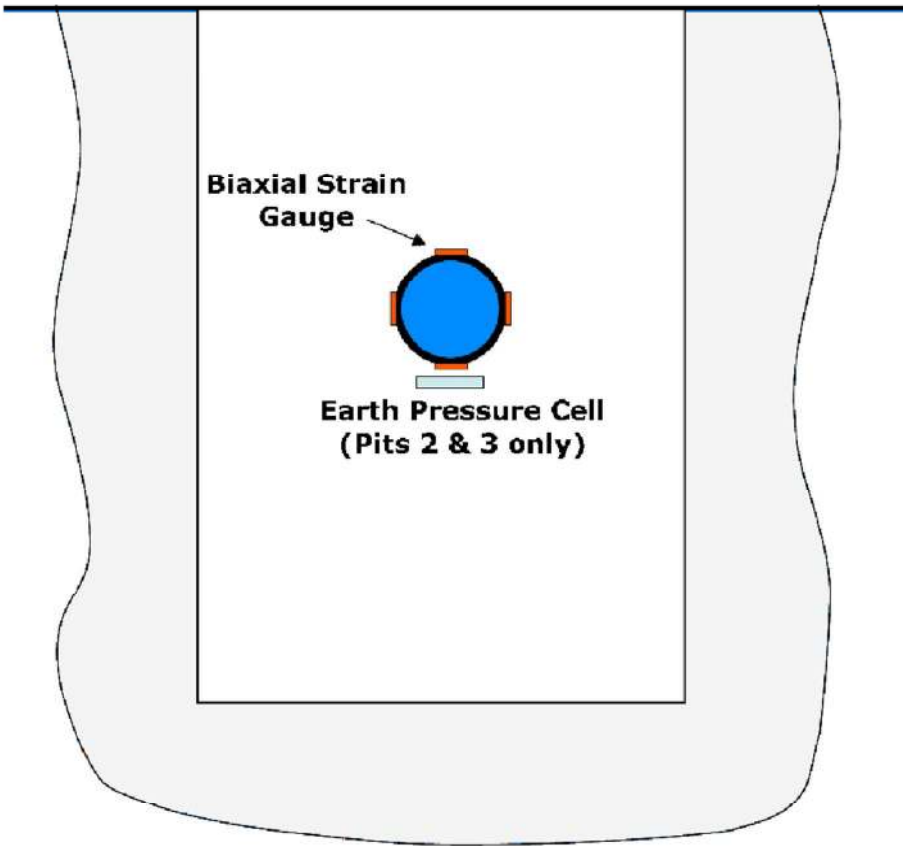


Fig. 7. Location of biaxial strain gauges around the pipe in a set 407x382mm (72 x 72 DPI)



Fig. 8. Installation of an earth pressure cell
708x294mm (72 x 72 DPI)

Draft

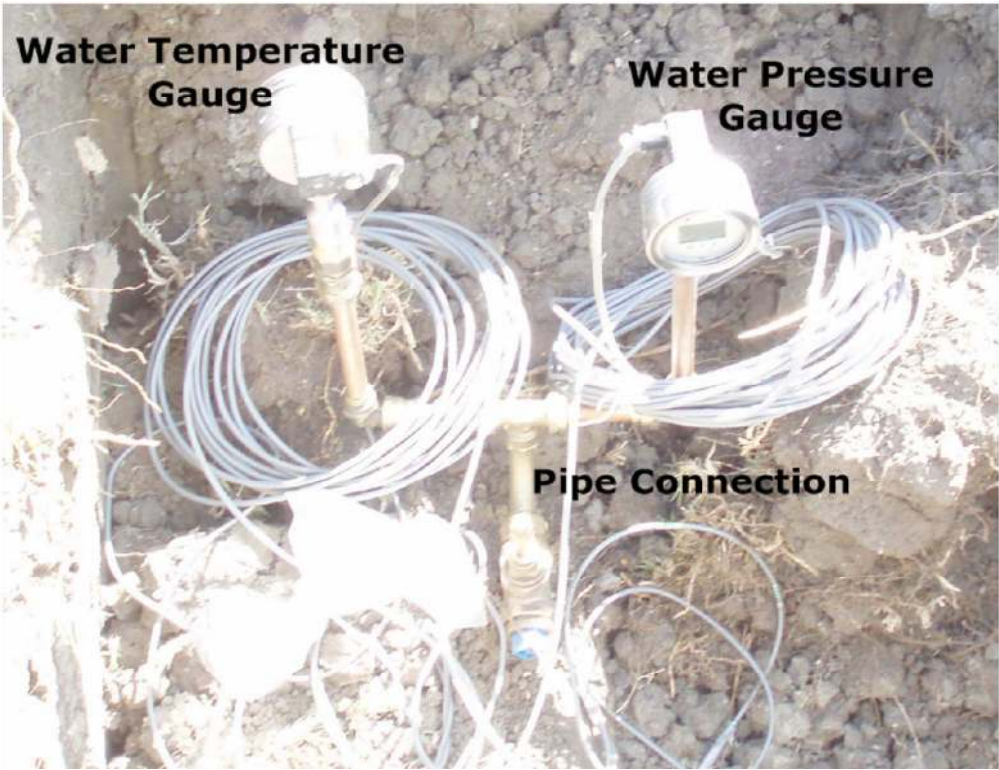


Fig. 9. Pipe water pressure and temperature gauges
352x270mm (72 x 72 DPI)

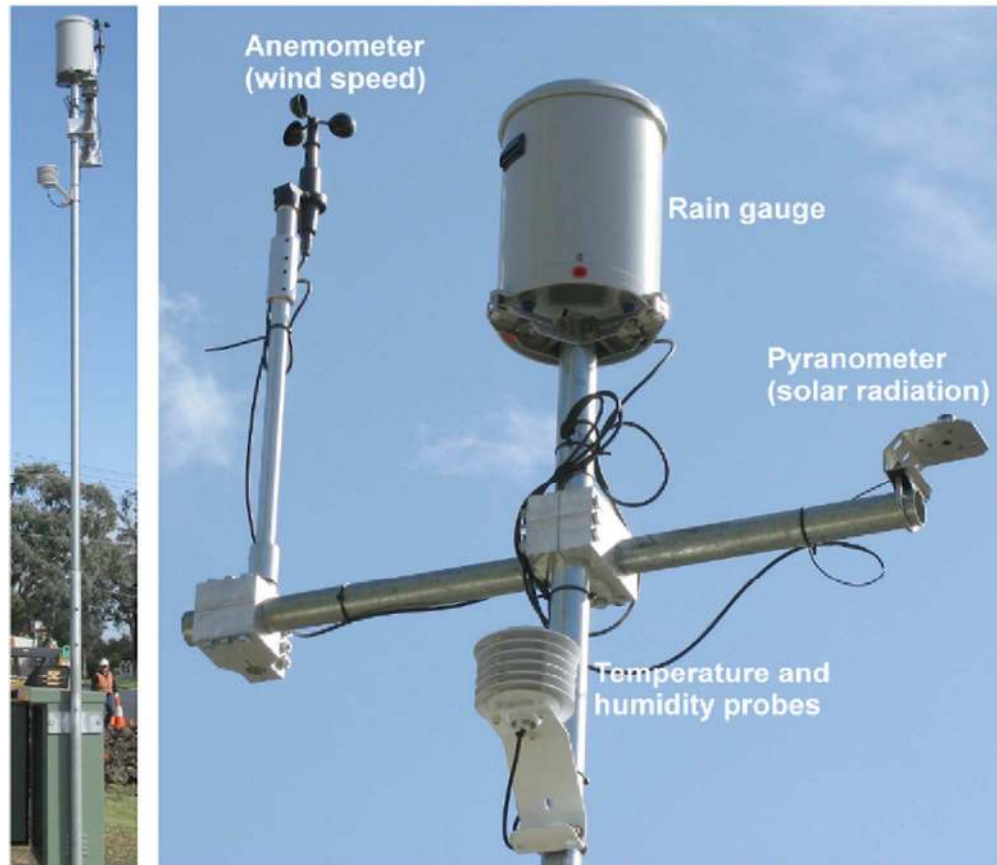


Fig. 10. Weather station and its components
282x243mm (72 x 72 DPI)

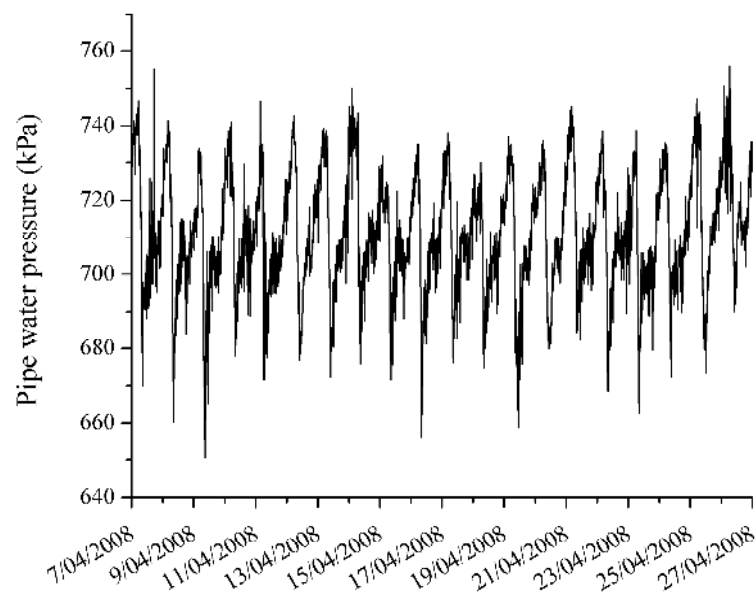


Fig. 11. Variation of pipe water pressure (collected in 10 min intervals)
1236x874mm (72 x 72 DPI)

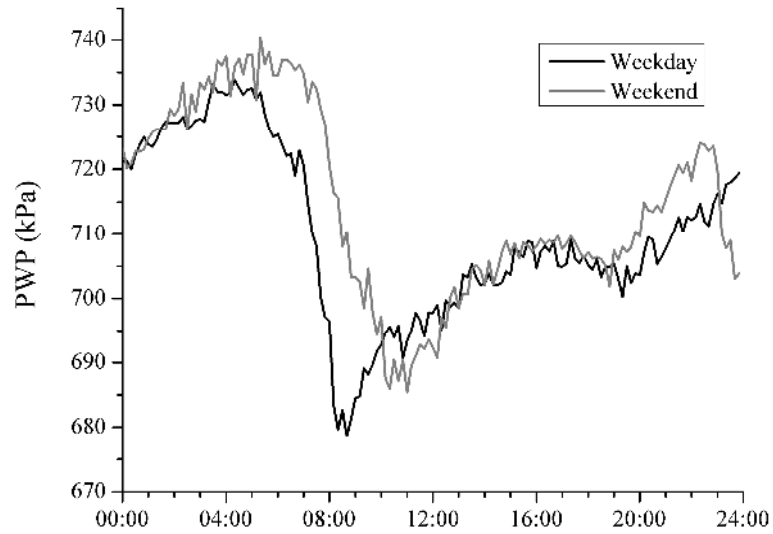


Fig. 12. Average daily fluctuation of pipe water pressure
1236x874mm (72 x 72 DPI)

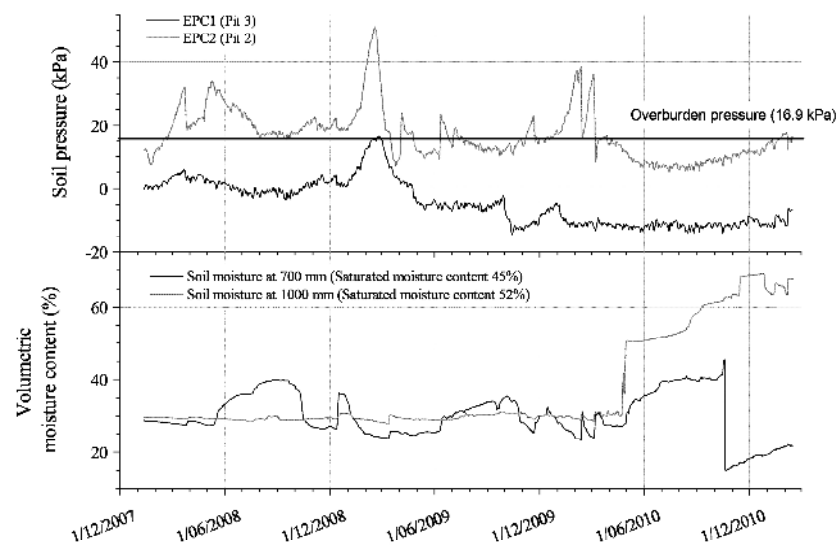


Fig. 13. Variation of soil pressure at Pit 2 and 3
297x209mm (300 x 300 DPI)

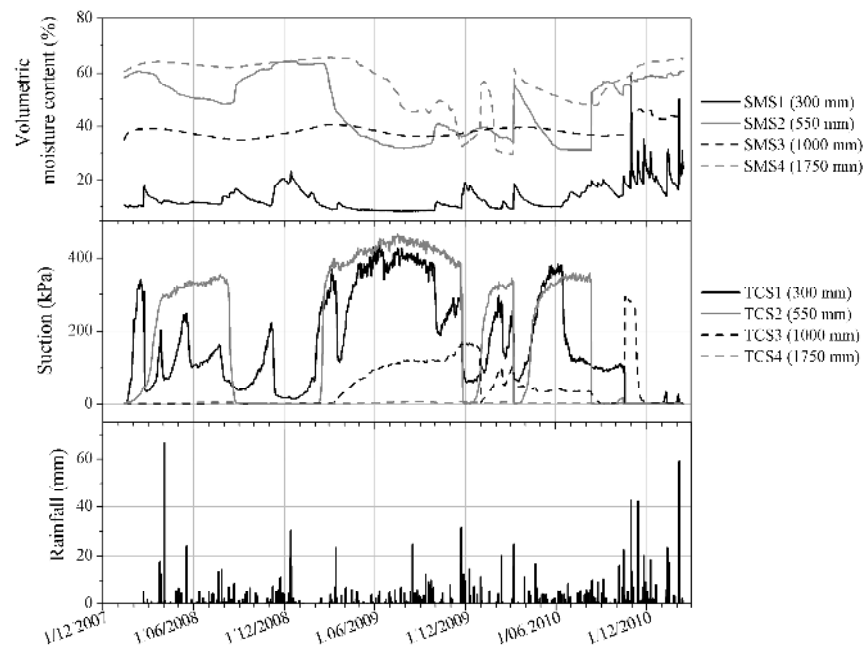


Fig. 14(a). The variation soil suction and moisture content in response to rainfall at Pit1
1236x874mm (72 x 72 DPI)

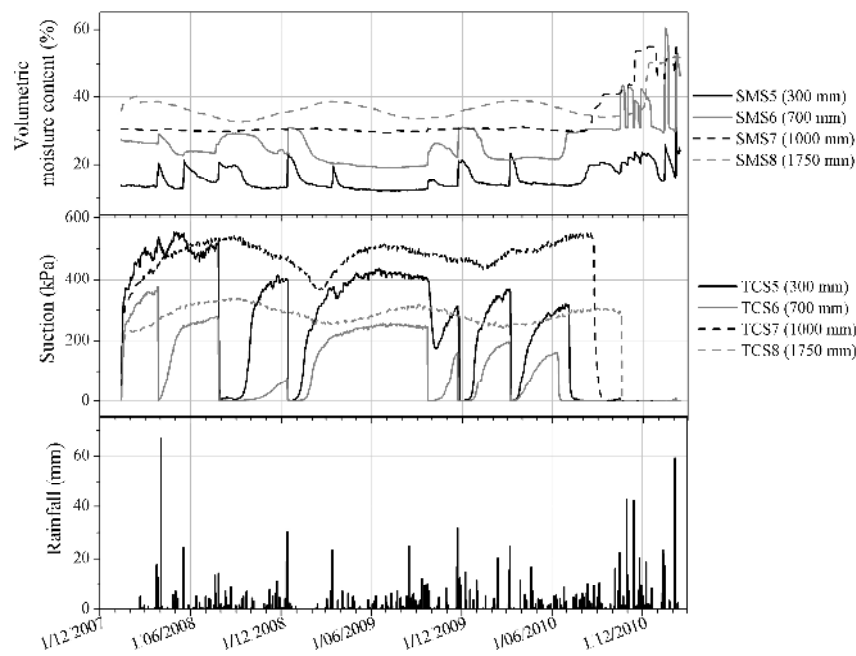


Fig. 14(b). The variation soil suction and moisture content in response to rainfall at Pit2
1236x874mm (72 x 72 DPI)

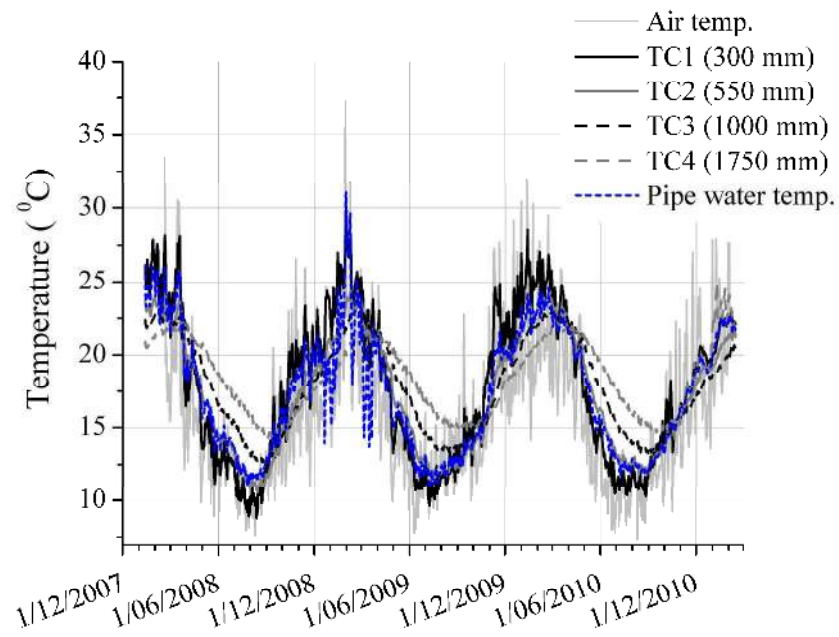


Fig. 15(a). Seasonal variation of soil temperature at Pit 1
1236x874mm (72 x 72 DPI)

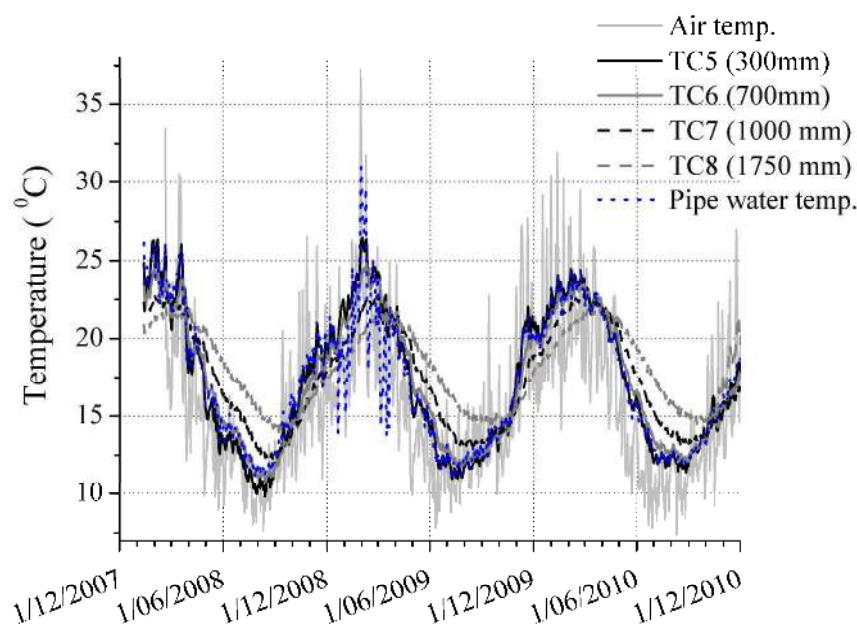


Fig. 15(b). Seasonal variation of soil temperature at Pit 2
1236x874mm (72 x 72 DPI)

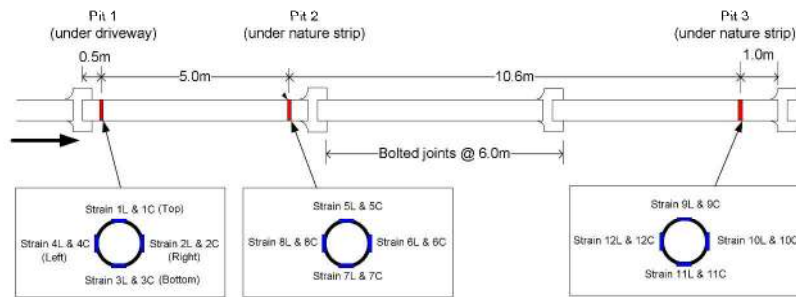


Fig. 16. Location and labelling of strain gauges on the pipe 1236x874mm (72 x 72 DPI)

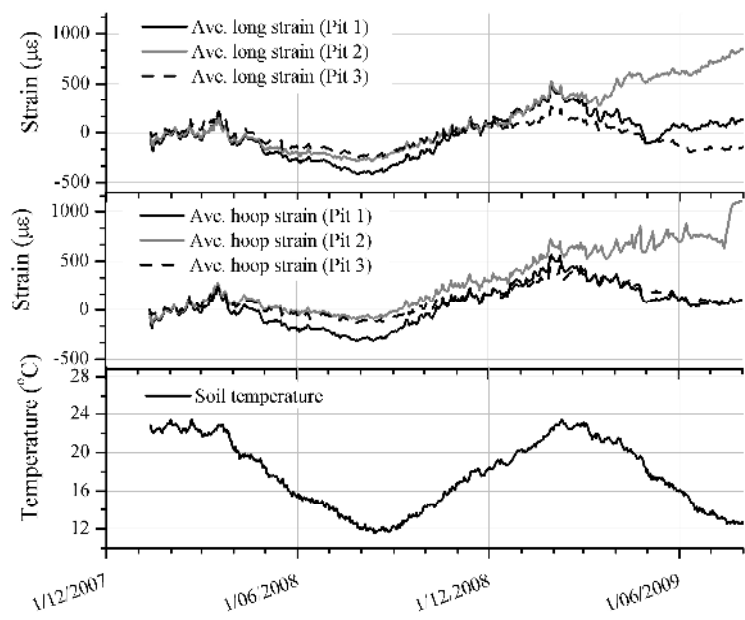


Fig. 17. Development of longitudinal and hoop strain in response to pipe temperature
1236x874mm (72 x 72 DPI)

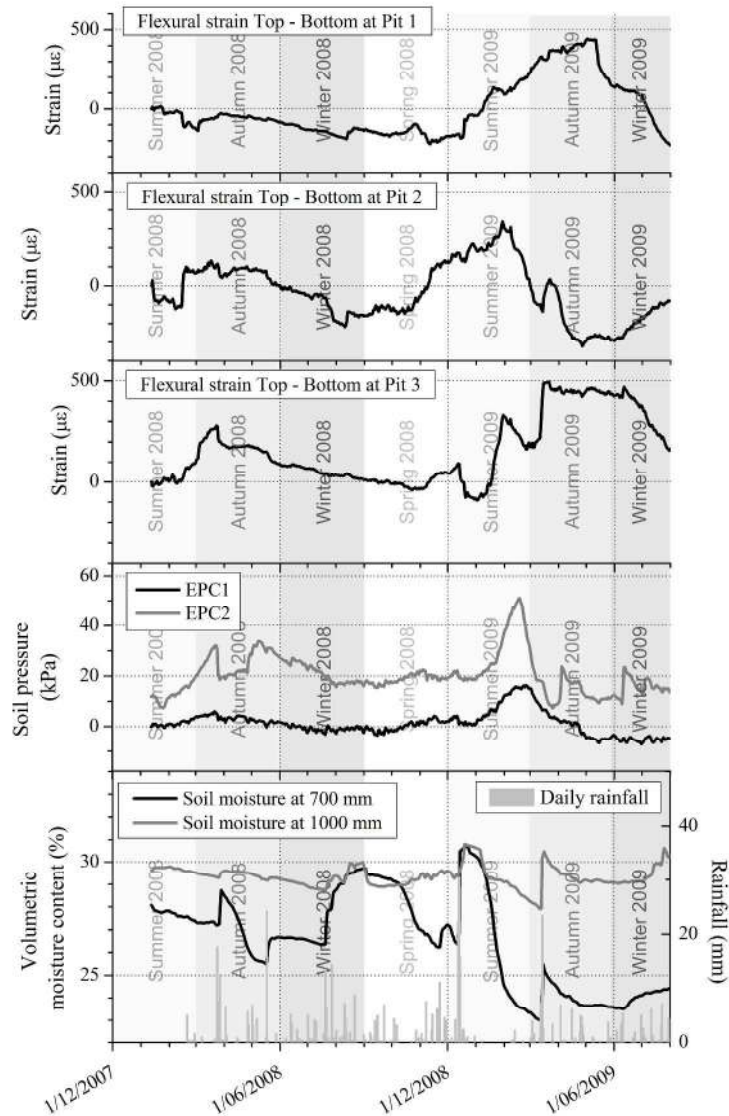


Fig. 18. Comparison of the difference between the top and bottom longitudinal strain gauges with soil pressure, displacement, moisture content and rainfall
260x391mm (300 x 300 DPI)

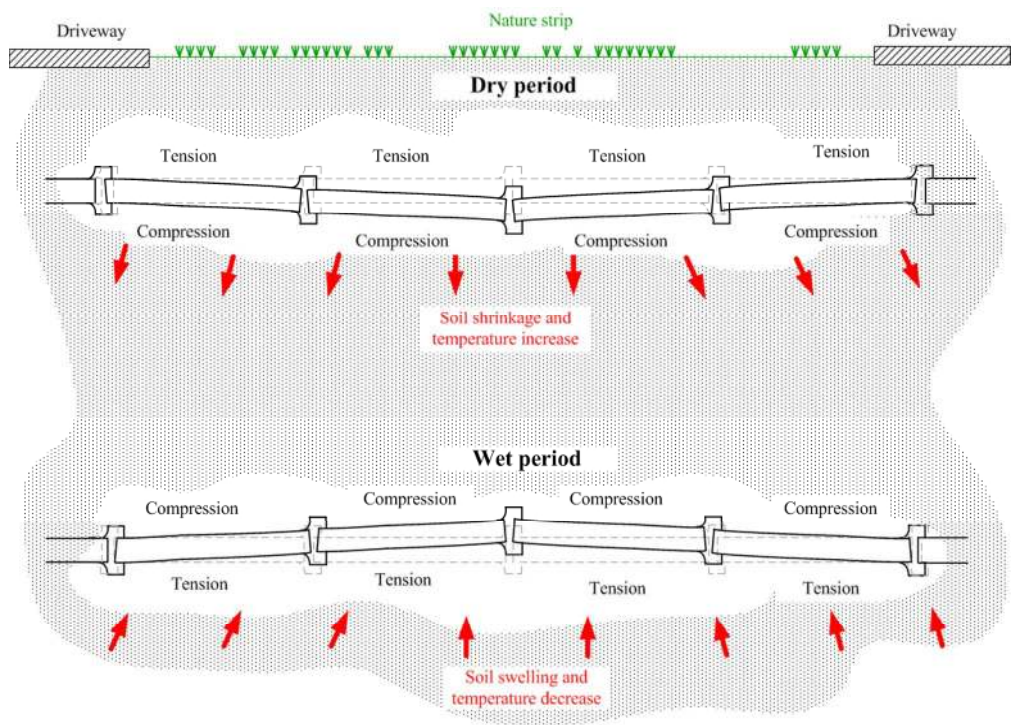


Fig. 19. Vertical pipe movement due to seasonal climate change of soil moisture content
280x201mm (96 x 96 DPI)

List of Tables

Table 1: Physical properties of field soil

Table 2: Mineralogy content of field soil

Draft

Table 1: Physical properties of field soil

Depth (mm)	LL* (%)	PL* (%)	PI* (%)	LS* (%)	Dry Density (g/cm ³)	Initial Water content ⁺ (%)	Swelling pressure (kPa)	Saturated hydraulic conductivity (m/2)	Texture	Soil classification
0 ~ 250	-	-	-	-	1.33	3.5 (26.4)	-	$5 \times 10^{-5} \sim 8 \times 10^{-6}$	Dark Brown	Top soil
250 ~ 500	72.0	27.8	44.2	21.7	1.46	21.4 (32.1)	205.8	1.9×10^{-9}	Brown	
500 ~ 750	87.3	29.5	57.8	24.0	1.53	23.7	551.8	-	Brown	Inorganic clays of high plastics
750 ~ 1000	99.4	28.9	70.5	21.2	1.50	24.4 (38.5)	371.2	1.1×10^{-9}	Brown	
1000 ~ 1300	91.2	23.4	67.8	26.6	1.58	25.1	412.1	-	Grey	
1300 ~ 2100	101.6	23.8	77.8	24.4	1.58	26.1 (30.8)	331.9	-	Light Brown	

*LL = Liquid Limit, PL = Plastic Limit, PI = Plasticity Index, LS = Linear Shrinkage

⁺Saturated water content shown within bracket

Table 2: Mineralogy content of field soil

Quartz	Albite	Orthoclase	Kaolin	Smectite	Calcite	Halite	Ilmenite	Anatase
59%	2%	3%	2%	31%	3%	<1%	-	<1%